






FULL PAPER

Efficient, rapid, and high-yield synthesis of aryl Schiff base derivatives and their in vitro and in silico inhibition studies of hCA I, hCA II, AChE, and BuChE

Musa Özil¹  | Halis T. Balaydın²  | Berna Dogan^{3,4}  | Murat Şentürk⁵  | Serdar Durdagi^{6,7} 

¹Department of Chemistry, The Faculty of Arts and Sciences, Recep Tayyip Erdogan University, Rize, Türkiye

²Education Faculty, Recep Tayyip Erdogan University, Rize, Türkiye

³Department of Chemistry, Istanbul Technical University, Istanbul, Türkiye

⁴Department of Biochemistry, School of Medicine, Bahçeşehir University, Istanbul, Türkiye

⁵Pharmacy Faculty, Agri Ibrahim Cecen University, Agri, Türkiye

⁶Computational Biology and Molecular Simulations Laboratory, Department of Biophysics, School of Medicine, Bahçeşehir University, Istanbul, Türkiye

⁷Molecular Therapy Lab, Department of Pharmaceutical Chemistry, School of Pharmacy, Bahçeşehir University, Istanbul, Türkiye

Correspondence

Murat Şentürk, Pharmacy Faculty, Agri Ibrahim Cecen University, 04100, Ağrı, Türkiye.
Email: msenturk@agri.edu.tr

Serdar Durdagi, Computational Biology and Molecular Simulations Laboratory, Department of Biophysics, School of Medicine, Bahçeşehir University, 34734 Istanbul, Türkiye.
Email: serdar.durdagi@bau.edu.tr

Funding information

Scientific Research Project Unit of Istanbul Technical University, Grant/Award Numbers: 44790, Grant Number: 44790; TÜBİTAK "Scientific and Technical Research Council of Turkey", Grant/Award Number: 112T640; Scientific Research Projects Commission of Bahçeşehir University, Grant/Award Number: BAP.2022-02.59 and BAP.2022-01.22

Abstract

This study reports a rapid and efficient synthesis of four novel aryl Schiff base derivatives. Biological activity and molecular modeling studies were conducted to evaluate the inhibitory effects of these compounds on human carbonic anhydrases (hCA) and cholinesterases. The results indicate that the triazole-ring-containing compounds have strong inhibitory effects on hCA I, hCA II, acetylcholinesterase (AChE), and butyrylcholinesterase (BuChE) targets. Besides comparing the Schiff bases synthesized in our study to reference molecules, we conducted in silico investigations to examine how these compounds interact with their targets. Our studies revealed that these compounds can occupy binding sites and establish interactions with crucial residues, thus inhibiting the functions of the targets. These findings have significant implications as they can be utilized to develop more potent compounds for treating the diseases that these target proteins play crucial roles in or to obtain drug precursors with enhanced efficacy.

KEYWORDS

1,2,4-triazole, Alzheimer's disease, carbonic anhydrase, cholinesterase, Schiff base

This is an open access article under the terms of the [Creative Commons Attribution-NonCommercial-NoDerivs](https://creativecommons.org/licenses/by-nc-nd/4.0/) License, which permits use and distribution in any medium, provided the original work is properly cited, the use is non-commercial and no modifications or adaptations are made.

© 2024 The Authors. *Archiv der Pharmazie* published by Wiley-VCH GmbH on behalf of Deutsche Pharmazeutische Gesellschaft.

1 | INTRODUCTION

Carbonic anhydrases (CAs, EC 4.2.1.1) are a group of metalloenzymes that catalyze the formation of carbonic acid by combining carbon dioxide and water. These enzymes play crucial roles in many biological processes and have multiple isoenzymes with varying functions.^[1] Due to their importance, inhibitors of CAs are utilized as therapeutic agents for various diseases, such as glaucoma, cancer, and epilepsy.^[1-3] The effect of many different small organic molecules on human CA isoenzymes has been previously investigated in different scientific studies.^[4-8] The use of CA inhibitors in the treatment of Alzheimer's disease (AD) is an area of ongoing research and investigation. While the primary focus of AD treatment has been on cholinesterase (ChE) inhibitors, the potential role of CA inhibitors in AD therapy is being explored due to their effects on brain function and neuroprotection. CA is an enzyme that plays a crucial role in maintaining acid–base balance and regulating pH in various tissues, including the central nervous system (CNS). In AD, there is evidence of altered CA activity and expression in affected brain regions, suggesting potential involvement in the disease process. Dysregulation of CA activity can affect various cellular processes, including neuronal function, synaptic activity, and cerebral blood flow, which are all implicated in AD pathology. By targeting CA, inhibitors have the potential to modulate neuronal activity, restore normal pH levels, and improve cerebral blood flow. These effects could have several potential benefits in AD. CA inhibitors may have direct neuroprotective effects by preserving neuronal integrity and preventing neuronal damage caused by oxidative stress, inflammation, and excitotoxicity, which are prominent features of AD. AD is associated with reduced cerebral blood flow, which can impair neuronal function and contribute to cognitive decline. CA inhibitors may improve blood flow by regulating vascular tone and enhancing oxygen amount and nutrient delivery to the brain. CA inhibitors might indirectly modulate neurotransmitter systems by influencing pH levels and ion transport in the synaptic cleft. This modulation could potentially impact cognitive function and memory processes affected in AD. While the potential benefits of CA inhibitors in AD treatment are promising, there are still several challenges to overcome: (i) Developing CA inhibitors that selectively target specific CA isoforms in CNS while avoiding off-target effects in other tissues is a challenge. (ii) Side effects related to systemic pH changes and electrolyte imbalances need to be carefully evaluated. (iii) Clinical trials investigating CA inhibitors in AD are limited and have yielded mixed results. CA inhibitors are likely to be used in combination with other therapies, such as ChE inhibitors or anti-inflammatory agents, to provide a multitargeted approach to AD treatment. The potential interactions and synergistic effects of these combinations need to be studied. Overall, the development of CA inhibitors has provided valuable insights into the role of CA enzymes in various physiological processes and has paved the way for potential therapeutic applications in conditions where pH regulation and bicarbonate/ion exchange are involved.

AD is a progressive neurodegenerative condition characterized by the deterioration of cognitive abilities, memory loss, and abnormal behaviors. It has emerged as a significant public health concern, particularly in developed nations with aging populations.^[9-11] Extensive research conducted on brain tissues from AD patients has uncovered notable differences in the levels of acetylcholine (ACh) and butyrylcholine (BCh), which are crucial neuromediator molecules, when compared with healthy brains. For this reason, compounds that can inhibit acetylcholinesterase (AChE) and butyrylcholinesterase (BuChE) enzymes that hydrolyze ACh and BCh molecules have become an option in the treatment of AD.^[11] As a result, many researchers globally have explored ChE inhibitors for AD treatment. Drugs such as donepezil, neostigmine, and rivastigmine are commonly employed due to their ability to inhibit AChE and BuChE enzymes, consequently increasing the concentration of crucial neurotransmitters, that is, ACh in the synaptic cleft. By elevating these neurotransmitter levels, these medications aim to enhance neurotransmission and alleviate the cognitive symptoms associated with AD.^[9,11,12] This cholinergic approach has demonstrated some effectiveness in managing the symptoms and slowing down the progression of the disease.

In the field of medicinal chemistry, triazoles, a class of nitrogen-containing heterocyclic molecules, have gained significant interest, which are found in the structures of many drugs used to treat various diseases. For example, fluconazole, ribavirin, anastrozole, vorozole, voriconazole, and letrozole contain the 1,2,4-triazole ring. It has been discovered that molecules with this cyclic structure have a wide range of pharmaceutical applications^[13] such as analgesic,^[14] anti-inflammatory,^[15] antifungal,^[16] and antitumor.^[17] The presence of the triazole pharmacophore provides these compounds with chemical diversity, making them valuable in medicinal chemistry research. Researchers continue to explore the therapeutic potential of triazoles and their derivatives in various disease areas, including neurodegenerative disorders like AD.

Recently, there has been a significant focus on the use of microwave technology for synthesizing heterocyclic compounds, due to its higher yield, easier clean-up, and improved reaction rate.^[18,19] As an eco-friendly approach, this method has distinctive advantages.^[20,21] In the current study, we bring out a synthesis method of cyclic triazoles containing homogeneous groups at N-2 and N-4 nitrogen atoms, such as Schiff bases, esters, and hydrazides. We assessed the yields and reaction rates of all reactions using both microwave and conventional methods.

ChEs play a crucial role in memory and cognitive processes, and any disruption in their balance can cause a decline in neural communication, ultimately leading to AD. AChE and BuChE are responsible for the hydrolysis of ACh, which results in reduced neural communication between nerve cells. This impairment leads to a decline in brain function, eventually manifesting as AD. Thus, maintaining a proper level of ACh is essential for treating AD. Numerous pharmaceutical studies have focused on developing

cholinesterase inhibitors (ChEIs) to address diseases associated with cognitive impairment.^[22–24] However, current AD drugs have limitations in terms of bioavailability and often cause undesired side effects such as gastrointestinal disorders. Consequently, there is a need for the development of new ChEIs that can overcome these drawbacks.^[25]

Oxidative stress has been linked to the pathology of AD. Changes in protein function, including their catalytic activity, can result from oxidative-induced protein modifications. The reduction in CA enzyme activity, including human carbonic anhydrase (hCA) II, has been noticed in brain samples from AD hippocampus and those with mild cognitive decline.^[26] Moreover, the identification of CA II among a large number of abundant plaque proteins suggests that it may play a central role in plaque development or co-occur with plaque formation.^[26]

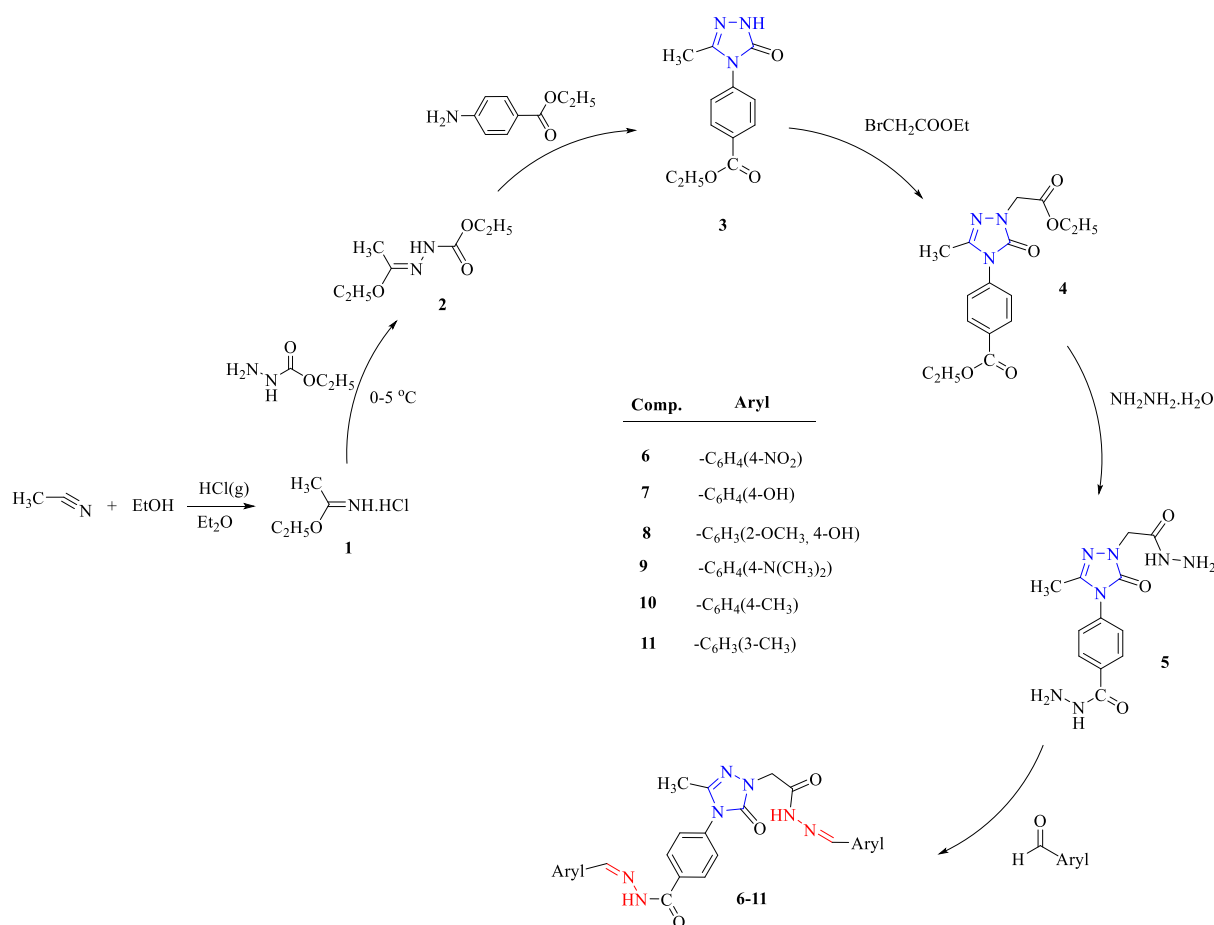
This study focuses on the synthesis of novel Schiff base derivatives to identify potential ChEIs. The synthesized compounds are subjected to evaluation to determine their effectiveness against two purified CA isoenzymes (hCA I and hCA II) derived from human erythrocytes, as well as AChE and BuChE. Furthermore, molecular modeling techniques are employed to examine how these ligands affect the structural and dynamic characteristics of the binding pockets in the target enzymes.

2 | RESULTS

2.1 | Chemistry

The synthetic path was started with the reaction of commercially available acetonitrile with ethanol and hydrochloric acid (gas form) to produce ethyl acetimidate hydrochloride (**1**) using the Pinner method.^[19] Then, ethyl acetimidate hydrochloride (**1**) was reacted with the hydrazinocarboxylic acid ethyl ester at 0–5°C to obtain ethyl 2-(1-ethoxyethylidene)hydrazinecarboxylate (**2**).^[18] The cyclization reaction occurred between ethyl 4-aminobenzoate and compound **2** to produce compound **3**, which is named ethyl 4-(3-methyl-5-oxo-1,5-dihydro-4*H*-1,2,4-triazole-4-yl)benzoate by using microwave technique under solvent-free condition.^[25] Afterward, ethyl-4-[1-(2-ethoxy-2-oxoethyl)-3-methyl-5-oxo-1,5-dihydro-4*H*-1,2,4-triazol-4-yl]benzoate (**4**) was obtained by the reaction of compound **3** with ethyl bromoacetate under both conventional and microwave irradiation techniques. In the penultimate reaction, compound **4** reacted with excess hydrazine hydrate to produce compound **5**, which has two identical hydrazide groups as described in the literature.^[20]

1,2,4-Triazole, 1,3,4-thiadiazole, or 1,3,4-oxadiazole derivatives were obtained from different reaction conditions by hydrazide



SCHEME 1 Synthesis route of 1,2,4-triazole derivatives.

compounds. Thus this structure can be regarded as a multifaceted group leading to the formation of many heterocycle systems.^[27] Moreover, hydrazide derivatives are compounds prone to react with different kinds of aldehydes producing Schiff bases. In this study, we aimed to synthesize the pharmacologically active 4-[1-(2-[4-(substitute)benzylidene]hydrazino)-2-oxoethyl)-3-methyl-5-oxo-1,5-dihydro-4H-1,2,4-triazol-4-yl]-N'-[[4-(substitute) phenyl]methylene] benzohydrazide (**6–11**) derivatives from the reaction of compound **5** with various aromatic aldehydes in the presence of acetic acid as a catalyst (Scheme 1). The reaction was carried out by two different techniques. As we concluded from the results, microwave irradiation is practicable and convenient for this reaction. The reaction yields (86%–94%) and reaction time (5 min) for the microwave irradiation technique were found more advantageous than the conventional technique (i.e., 70%–83%) yield and 12 h reaction time. Microwave irradiation heating comes up with more advantages, such as reduced pollution, high yield, simplicity in processing, reduced reaction time, and low cost.

2.2 | Biological activity studies

This study reports the inhibition activities of a total of six Schiff base derivatives (**6–11**), four of these compounds are newly synthesized (**8–11**), on hCA I, hCA II, AChE, and BuChE enzymes (Table 1).

Structure–activity relationships (SAR) of studied compounds are provided below:

- (i) Compounds **6–11** were tested for the hCA I enzyme. The IC_{50} values of these substances were determined to be between 0.0435 and 0.2374 μ M. When the IC_{50} values of the tested substances were compared with the reference molecule acetazolamide (AZA),

TABLE 1 hCA I, hCA II, AChE, and BuChE inhibition data of the synthesized compounds.

Inhibitor	IC_{50} (μ M)*			
	hCA I	hCA II	AChE	BuChE
6	0.0435	0.0402	0.0587	0.0614
7	0.0724	0.0694	0.0613	0.0596
8	0.0512	0.0483	0.0608	0.0684
9	0.2374	0.2166	0.0412	0.0538
10	0.0984	0.0953	0.0515	0.0637
11	0.0973	0.0877	0.0538	0.0609
Acetazolamide (AZA) ^a	0.9925	0.4848	–	–
Neostigmine	–	–	0.136	0.0840

Note: *The values shown in the table are the average of at least three measurements. An error rate of $\pm 3\%$ of the stated value was determined (data not shown).

Abbreviations: AChE, acetylcholinesterase; BuChE, butyrylcholinesterase; hCA, human carbonic anhydrases.

^aMete et al.^[28]

it was determined that they were effective inhibitors. It has been shown that the most effective compound among the tested is **6**, which contains the 4-nitro benzene group. When we compared these substances among themselves, it was determined that it was compound **9** containing the 4-(dimethylamino)benzylidene functional group. Similar results were obtained for many substances, such as sulfonamides, uracil derivatives, natural molecules, and so on, in different previous kinetic studies on the hCA I enzyme.^[29–34]

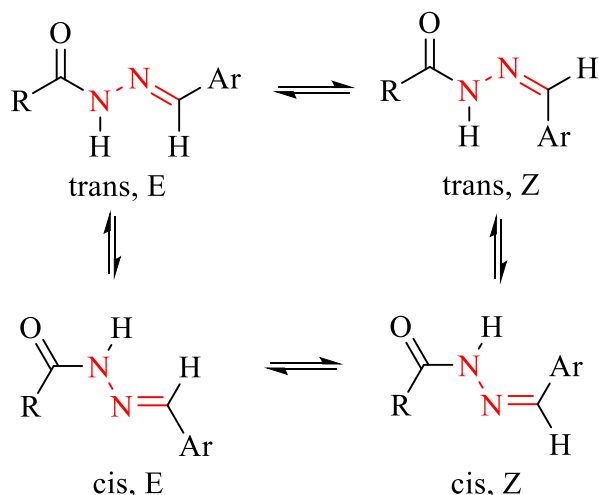
- (ii) Compounds **6–11** were tested for the hCA II enzyme. The IC_{50} values of these substances were determined to be between 0.0402 and 0.2166 μ M. When the IC_{50} values of the tested substances were compared with the reference molecule AZA (IC_{50} : 0.4848 μ M), it was determined that they were effective inhibitors. It was observed that compounds **6** and **8** were the most effective molecules. When we compared these items among themselves, it was determined that compound **9** was the one with the weakest biological effect. Similar results were obtained for many substances, such as sulfonamides, uracil derivatives, natural molecules, and so on, as in hCA I, in different previous kinetic studies on the hCA II enzyme.^[29–33]
- (iii) Compounds **6–11** whose inhibitory activities against AChE enzyme were examined (IC_{50} values of these substances were determined to be between 0.0412 and 0.0613 μ M), the weakest active compound was determined as **7** (IC_{50} = 0.0613 μ M). We determined that compound **9**, which contains 4-(dimethylamino) phenyl as a functional structure in the aryl group, is the most effective molecule. Similar results were also obtained for different substances in the literature.^[25,30] The IC_{50} values of studied compounds obtained for the AChE enzyme were observed to be better when compared with the reference molecule neostigmine (IC_{50} : 0.136 μ M).
- (iv) The IC_{50} values obtained for six compounds tested with the BuChE enzyme were determined between 0.0538 and 0.0684 μ M, with compound **8** (IC_{50} = 0.0684 μ M) showing the weakest inhibitory effect. We determined that compound **9** (IC_{50} : 0.0538 μ M) was the most effective. The fact that the dimethylamine (similar to triethylamine in ACh) group of compound **9** has a stronger inhibitory capacity as a functional group may indicate that its geometry is stronger to interact with the enzyme active site. Similar results of different substances in literature are available.^[25,30] Results show that the values obtained for the BuChE were better than the reference molecule neostigmine (IC_{50} : 0.084 μ M).

Over the past few decades, numerous studies have demonstrated that phenolic or polyphenolic compounds possess inhibitory properties comparable to sulfonamides, which are recognized as potent CA inhibitors.^[35] This finding presents a promising avenue and a new class of inhibitors that could be beneficial for individuals with sulfonamide allergies, particularly in the context of treatment regimens.^[29–33,35–37] Research conducted by various groups, including our own, has established that certain heterocyclic molecules, particularly those containing electronegative atoms within their

molecular structures, exhibit significant CA inhibitory effects akin to phenolic compounds and sulfonamides. These findings have shed light on their potential relevance to disease and their possible application in disease treatment.^[3-5,8] Furthermore, our investigations have revealed that the tested substances, capable of inhibiting both CA and ChE enzymes, hold promise as potential therapeutic candidates for the treatment of AD. In addition to experimental studies, computational simulations were performed to elucidate the quantitative relationships between the molecular structure of these compounds and their activity, thus providing valuable insights into SAR. These findings provide a foundation for further exploration and development of novel inhibitors targeting both CA inhibition and ChE inhibition, with potential implications for the treatment of AD and other related conditions.

2.3 | Molecular modeling studies

All the compounds synthesized in this study contained two double bonds that have different groups attached, which enable geometric isomer pairs: *E,E*, *E,Z*, *Z,E*, and *Z,Z* forms. Previous studies^[37-39] have shown that the binding modes of these geometrical isomers could be different. Based on nuclear magnetic resonance (NMR) data for synthesized compounds, *E* isomers are favored but there is a mixture of isomers for all compounds. Additionally, due to the amide bonds in the structures, there is restricted rotation around the HN-C=O linkage and *cis/trans* forms of isomers could be generated, as shown in Scheme 2. NMR spectrum of compounds indicated that compounds exist as mixtures of *cis/trans* as well as *E/Z* isomers with *cis* form and *E* isomers being favored. However, it must be noted that when forming complexes with the targets, amide bonds could flip. As a result, *trans* isomer binding is preferred even though *cis* isomer is the one favored in the solution, that is, when the ligand is not located to the targets.



SCHEME 2 Representation of *cis/trans* isomers and *E/Z* geometrical isomers for the synthesized compounds 6–11.

During molecular docking, with the ligand flexibility option, it is possible to flip amide bonds and generate *cis/trans* isomers for amide groups. However, it is not possible to generate *E/Z* geometric isomers with ligand flexibility options during docking. As such, we have generated four geometric isomers for each of the compounds tested in vitro assays and considered these isomers to be different compounds for molecular docking. However, we did not specifically generate *cis/trans* for each compound but allowed these amide bonds to flip if appropriate during docking simulations. In the end, we have selected the isomers for amide bonds with the highest docking scores for each target and each isomer. We named *E/Z* isomers depending on the relative positions of chemical groups attached to A and B double bonds (shown in Supporting Information S1: Figure S1). Compounds are named based on first the A bond isomerization state and then the B bond isomerization state. Additionally, reference compounds considered in vitro studies, Neostigmine and AZA were also prepared for molecular docking and molecular dynamics (MD) simulations studies. All compounds with isomerization states treated as different compounds were docked into the binding sites of target proteins considered in the study: hCA I, hCA II, AChE, and BuChE. GOLD (Genetic Optimization for Ligand Docking) docking program with CHEMPLP (Piecewise Linear Potential) scoring function was utilized in which higher scores indicate better docking poses and results. The top docking scores for each compound and its isomers are displayed in Supporting Information S1: Table S1. The top docking poses obtained for each compound/isomer were also subjected to MD simulations and binding free energies were calculated by molecular mechanics/generalized Born surface area (MM/GBSA) method for protein–ligand complexes. The average MM/GBSA binding free energies are displayed in Supporting Information S1: Table S2.

Both hCA I and hCA II are metalloenzymes that contain Zn^{2+} ions and the inhibitors for them could have different binding modes depending on their mechanism of action as well as the region they occupy.^[35,40] While inhibitors such as sulfonamide derivatives bind to Zn^{2+} , others could interact with water molecules coordinated with Zn^{2+} or even occupy the entrance of active cavities without interacting with Zn^{2+} or coordinated water like coumarin. Here, we chose the binding sites for docking such that both the active and entry sites were considered. Additionally, we employed crystal structures that already have a coordinated water molecule to the Zn^{2+} ion but allowed the water molecule to switch on/off during docking so that compounds if appropriate could bind to the ion. It is observed that all the molecules could fill the exit of the active site cavity (where coumarins usually bind)^[41-43] while some of them could also extend into the active site. Also, all the molecules studied here are considerably larger than usual inhibitors of hCA I and II target proteins (e.g., phenol, sulfonamide, or coumarin derivatives) and therefore they could also form interactions with the other residues, specifically with the ones closer to the N terminus.

The reference compound AZA was also docked into the binding cavity, and the docking algorithm employed was able to reproduce the binding pose of AZA with coordination to the Zn^{2+} ion. MD

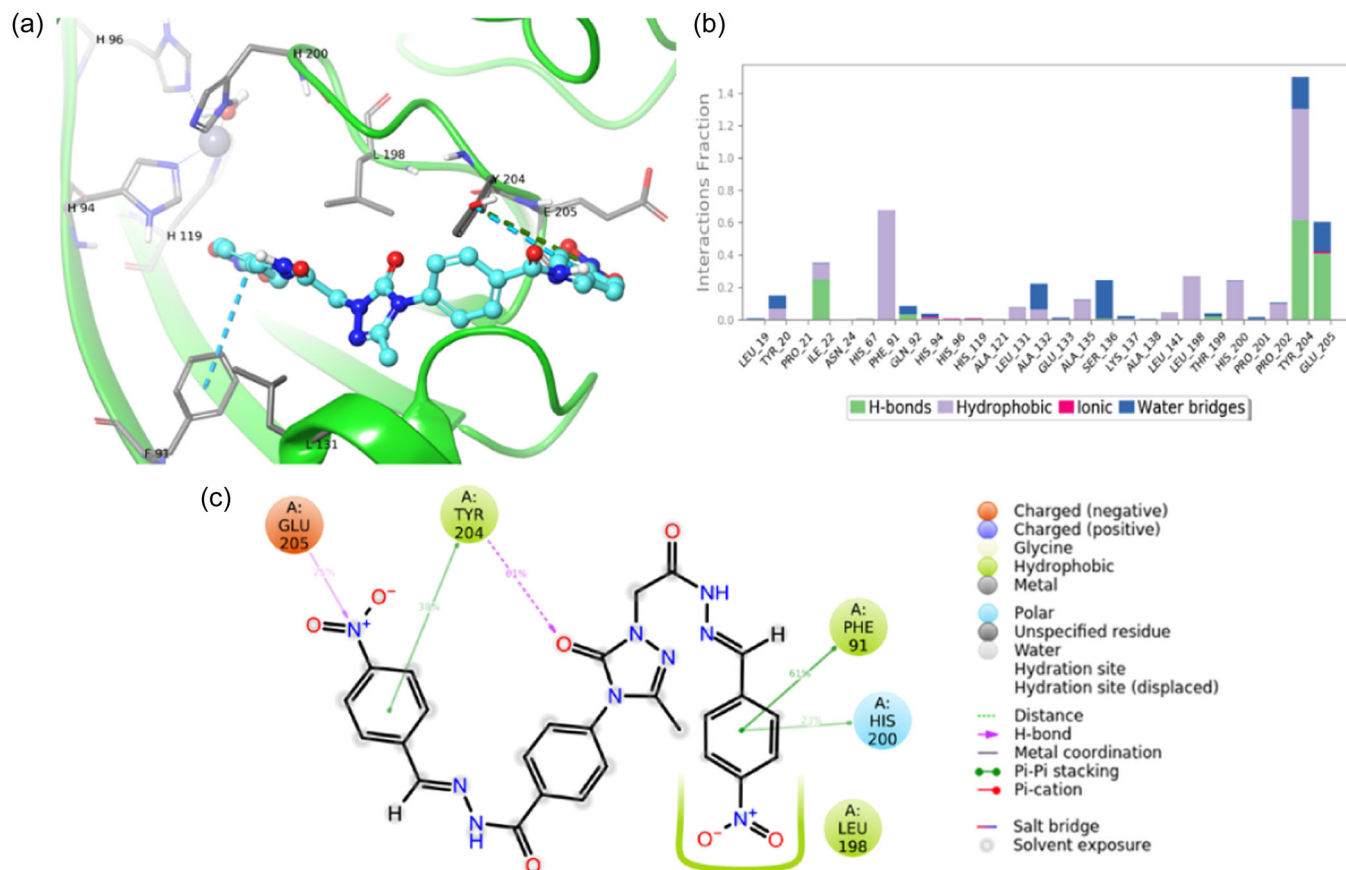


FIGURE 1 Interactions of compound **6** isomer *E,E* with human carbonic anhydrases (hCA) I. (a) Representative three-dimensional (3D) structure of compound **6** at the binding site with dashed cyan lines demonstrating π - π stacking interactions and yellow dashed lines hydrogen bonding interactions. Zn^{2+} coordination bonds are displayed as gray-blue dashed lines. (b) Normalized interaction fractions of compound **6** with target as histogram. (c) A diagram showing the two-dimensional (2D) interactions between a protein and ligand, with percentages indicating the stability of the interactions observed over the simulation period.

simulations as well as MM/GBSA analysis of compound-target complexes for the poses with the best scores were performed as mentioned. All compounds have lower inhibition constants compared with reference AZA though some molecules are considerably more promising compared with others such as **6** and **8** with the lowest inhibition constants. Based on MM/GBSA results, again these compounds have relatively lower free energy (FE) of binding compared with AZA, that is, more negative MM/GBSA scores. Hence, we have focused on the interaction of these compounds with target proteins.

Specifically, it was critical to investigate how persistently these interactions were observed during MD simulations. Figures 1 and 2 display these interactions for compounds **6** and **8** with target human carbonic anhydrase (hCA) I. *E,E* isomer of compound **6** was the isomer with the most favorable FE and in the binding pose, one of the amide bonds had *cis* conformation (next to the B bond displayed in Supporting Information S1: Figure S1) while the other one was observed to be in *trans* conformation. The isomer was surrounded by important residues, such as Phe91, Leu198, Thr199, His200, and Tyr204, though it did not interact with coordinated water molecules (Figure 1a). Persistent hydrogen bonds with Tyr204 and π - π

stacking interactions with Phe91 were observed (Figure 1b,c). For compound **8**, *E,Z* isomer was observed to be the one with the lowest FE among other isomers of this compound with both amide bonds having *trans* conformation in the binding pose at the cavity site of hCA I. In this case, compound **8-E,Z** bound to Zn^{2+} via the O atom of the hydroxy group (Supporting Information S1: Figure S2a). It was surrounded by important residues, such as Leu198, Thr199, His200, and Pro202, and formed lasting hydrogen bonds with Thr199 and π - π stacking interactions with His200 during MD simulations (Supporting Information S1: Figure S2b,c). At the binding site of hCA II, compound **6 E,E** isomer was determined as the isomerization state with the lowest FE, and in the binding mode, both amide bonds had *trans* conformation. The isomer though did not bind to the Zn^{2+} ion and was not directly interacting with coordinated water molecules, it occupied the entrance of the active cavity (Figure 2a). Additionally, it formed persistent hydrophobic interactions with N-terminus residue Trp5 (Figure 2b) and water-bridged interactions with Lys170 and Pro201 (Figure 2c). Compound **8** isomer with the most favorable FE at hCA II binding cavity was *Z,E* and in the binding mode, one of the amide bonds had *trans* conformation while the other one (next to the B bond displayed in

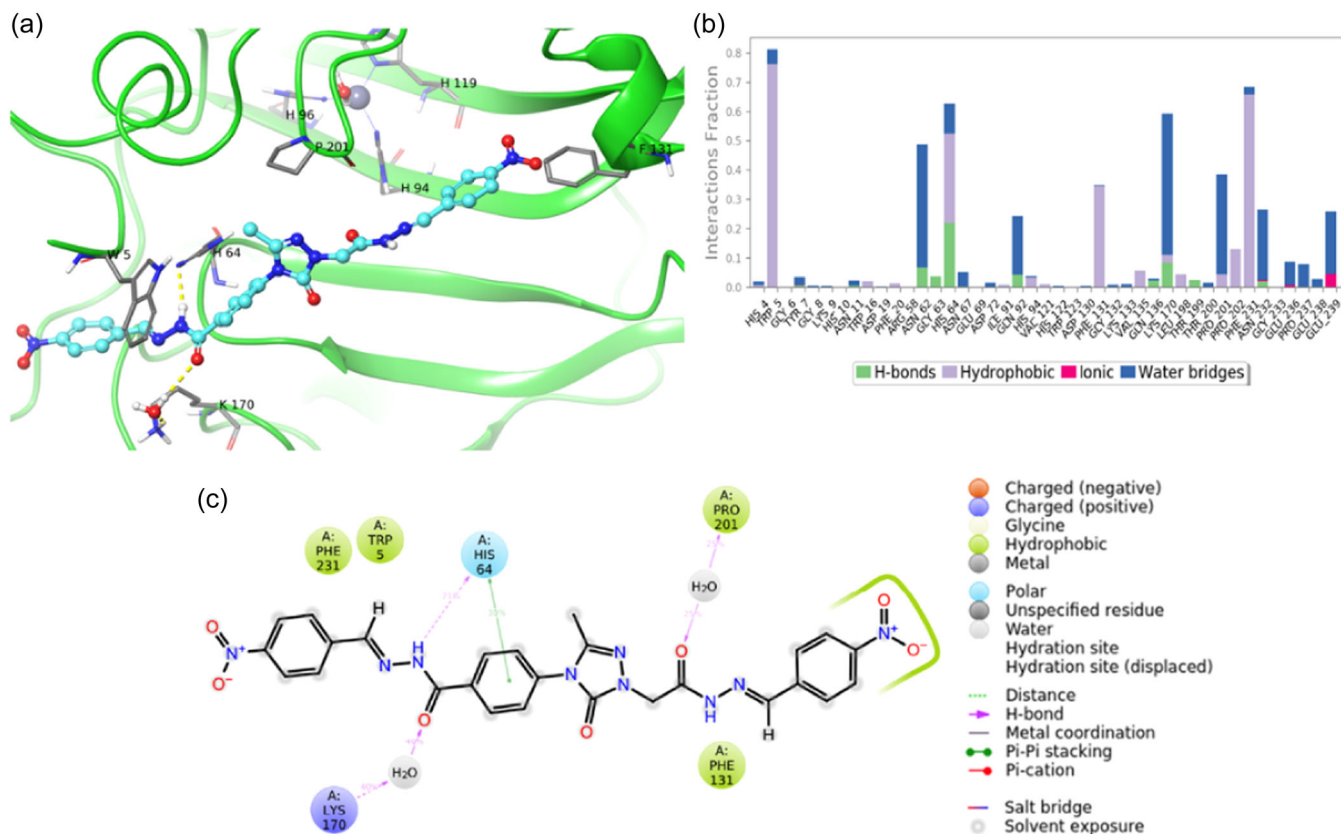


FIGURE 2 Interactions of compound 6 isomer *E,E* with human carbonic anhydrases (hCA) II. (a) Representative 3D structure of compound at the binding site with dashed cyan lines demonstrating π - π stacking interactions and yellow dashed lines hydrogen bonding interactions. Zn^{2+} coordination bonds are displayed as gray-blue dashed lines. (b) Normalized interaction fractions of compound with target as histogram. (c) A diagram showing the 2D interactions between a protein and ligand, with percentages indicating the stability of the interactions observed over the simulation period.

Supporting Information S1: Figure S1) was observed to be in *trans* conformation. Again, the isomer did not interact with Zn^{2+} or coordinated water molecules. However, it inhibited the entrance of the active cavity and was close to Phe131, a critical residue (Supporting Information S1: Figure S3a). This compound formed persistent hydrogen bonding interactions with Trp5, N-terminus residue, and hydrophobic interactions with Phe231 (Supporting Information S1: Figure S3b,c).

As can be seen from inhibition data, for ChE proteins (AChE and BuChE), the inhibition constants are quite similar for all compounds, and better inhibition constant values compared with reference molecule neostigmine are observed for almost all compounds. This can also be observed in the MM/GBSA results though the ranking of ligands could not be matched with the experimental trend as the differences between compound inhibition constants are negligibly small (Supporting Information S1: Table S2). Still, compound 9 was found to be the most promising *in vitro* as it has relatively lower IC_{50} values compared with neostigmine. Hence, we have chosen the poses for compound 9 isomers with the lowest FE, that is, most negative MM/GBSA scores for AChE and BuChE, and investigated the interactions this compound formed with targets. *E,E* isomer of compound 9 was

found to be the one with the most favorable FE of binding for AChE. In the binding mode, one of the amide bonds had *cis* conformation (close to the B bond displayed in Supporting Information S1: Figure S1) while the other one is observed to be in *trans* conformation. This isomer though not interacting with catalytic site residues (i.e., His447, Ser203, Glu334) was on the peripheral site of AChE that extends beyond Tyr337 and contains numerous aromatic side chains^[44] (Figure 3a).

In the binding mode, the isomer was surrounded by important residues, such as Trp286, Trp86, Ser293, Tyr337, and Phe295, and formed various persistent hydrogen bonding interactions with them (Figure 3b,c). Specifically, the hydrogen bond interaction with Phe295 was maintained fully during MD simulations. At the cavity of BuChE, the isomer of compound 9 with the most favorable FE of binding was *Z,E* and in the binding pose, both amide bonds were in *trans* conformation. The isomer was not directly interacting with catalytic site residues (His438, Ser198, Glu325), however, it was on a peripheral site surrounded by residues, such as Asn68, Asp70, Trp82, Ala277, and Val280 (Figure 4a). This isomer formed long-lasting hydrogen bonds with Ala277 and Val280 in addition to π - π stacking interactions with Trp82 (Figure 4b,c).

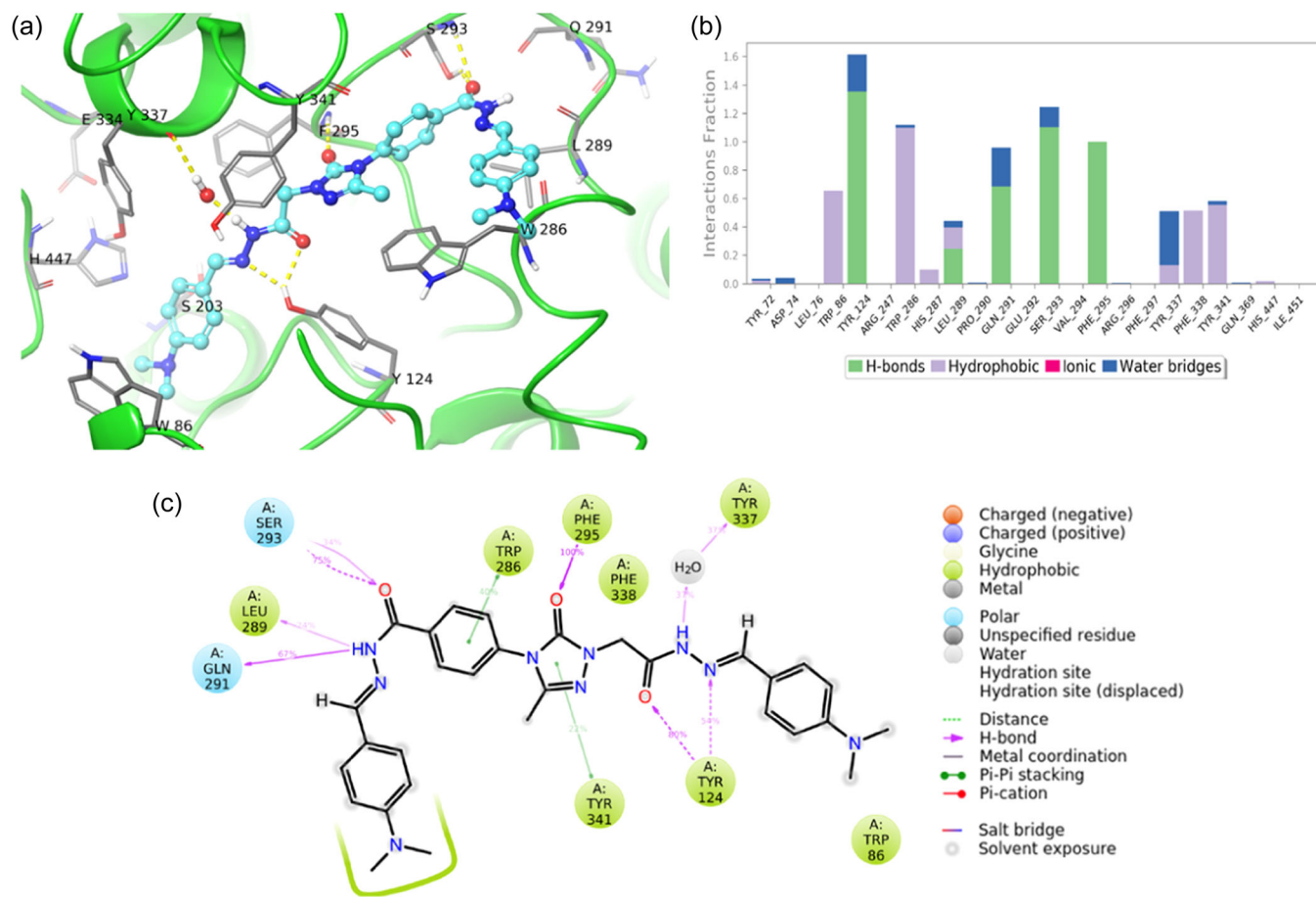


FIGURE 3 Interactions of compound **9** isomer *E,E* with acetylcholinesterase (AChE). (a) Representative 3D structure of compound at the binding site with dashed cyan lines demonstrating π - π stacking interactions and yellow dashed lines hydrogen bonding interactions. Zn^{2+} coordination bonds are displayed as gray-blue dashed lines. (b) Normalized interaction fractions of compound with target as histogram. (c) A diagram showing the 2D interactions between a protein and ligand, with percentages indicating the stability of the interactions observed over the simulation period.

3 | DISCUSSION AND CONCLUSIONS

AChE and BuChE inhibitors, as well as CA inhibitors, have been investigated for their potential role in the treatment of AD. AChE and BuChE are enzymes responsible for the hydrolysis of ACh and BCh, which are important neurotransmitters involved in cognitive functions. In AD, there is a decrease in ACh levels due to the excessive activity of these enzymes, leading to cognitive decline. These inhibitors work by blocking the activity of AChE and BuChE enzymes, thereby increasing the concentration of ACh in the CNS. By maintaining higher levels of ACh, these inhibitors can enhance neurotransmission and temporarily alleviate cognitive symptoms in AD patients. CA is an enzyme that catalyzes the conversion of carbon dioxide to bicarbonate and protons. In the brain tissues, CA is involved in maintaining pH balance and regulating neuronal activity. Alterations in CA activity have been observed in AD, suggesting its potential involvement in disease pathology. Research has explored the use of CA inhibitors as a potential therapeutic approach for AD. By targeting CA, these inhibitors aim to restore normal pH levels, enhance cerebral blood flow, and

modulate neuronal function. However, the exact mechanisms and potential benefits of CA inhibitors in AD treatment are still under investigation, and further studies are needed to determine their efficacy and safety. It is worth mentioning that while AChE, BuChE, and CA inhibitors have shown promise in preclinical and clinical studies, their effects on AD symptoms vary among individuals, and their long-term benefits remain a subject of ongoing research. These inhibitors are typically used in combination with other treatments, such as memantine (an NMDA receptor antagonist), to provide a comprehensive approach to managing AD symptoms.

The newly synthesized compounds were characterized by different spectral analyses (Supporting Information S1: Figures S4–S19). The results demonstrated that all data are coherent with our proposed compounds. The characteristic infrared (IR) stretching vibrations are seen at about 1590, 1677, and 1720 cm^{-1} related to C=N, C=O (hydrazide), and C=O (triazole) signals, respectively. Besides that, the $-\text{NH}_2$ signal of compound **5** was disappeared in the spectrum of compounds **6–11**, and new C=O signals were shifted from 1657 to 1677 cm^{-1} owing to consist of the imine group.

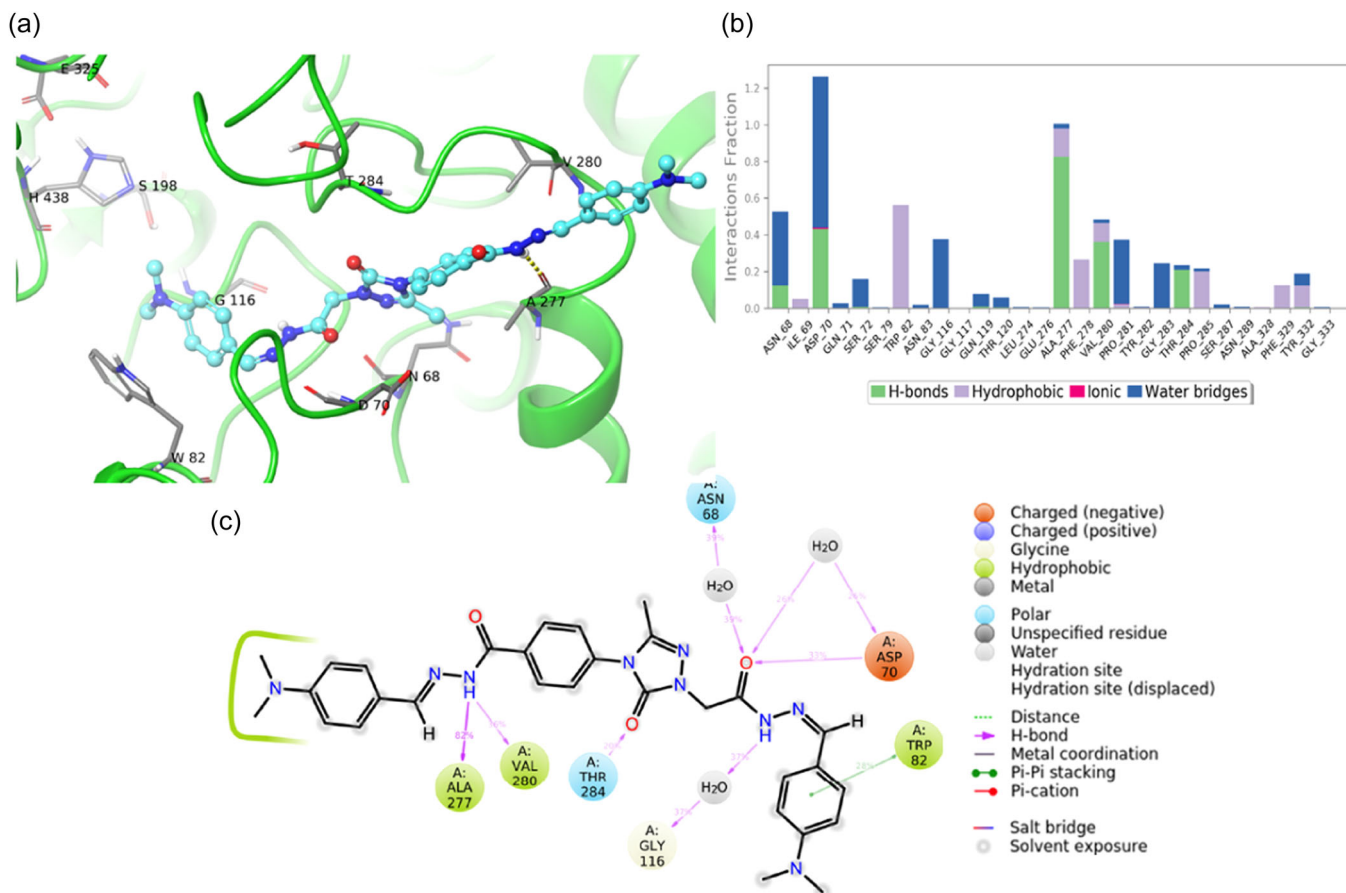


FIGURE 4 Interactions of compound **9** isomer *Z,E* with butyrylcholinesterase (BuChE). (a) Representative 3D structure of compound **9** at the binding site with dashed cyan lines demonstrating π - π stacking interactions and yellow dashed lines hydrogen bonding interactions. Zn^{2+} coordination bonds are displayed as gray-blue dashed lines. (b) Normalized interaction fractions of compound with target as histogram. (c) A diagram showing the 2D interactions between a protein and ligand, with percentages indicating the stability of the interactions observed over the simulation period.

When the NMR spectrum is examined for compounds **6–11**, a prominent N-H signal was seen at about 11.80 and 12.00 ppm. However, it must be noted that, in the ^1H -NMR spectra, some protons have two sets of signals at the different shifts of ppm for compounds **6–11**. Hydrazide-arylidene groups in the compounds, which exist as *E/Z* geometrical isomers from *cis/trans* amide conformers at the CO-NH single bond and C=N double bond. In the literature,^[45,46] C=N double bond would rather *E* geometrical isomer in $\text{DMSO}-d_6$ and *Z* isomers can be opted into a smaller extent solvent such as MeOD by an intramolecular H bond. All target compounds (**6–11**) have two sets of signals because of *cis/trans* conformers corresponding -NH-, -N=CH, and N-CH₂ groups in the ^1H NMR spectrum. The results show that the -NH signal has two sets because of *cis/trans* amide conformers at about 11.80 ppm and about 11.75 ppm. In addition, the -N=CH signal was observed as two sets due to the *E* and *Z* geometrical isomers at about 8.30 and about 8.19 ppm, respectively. The upfield lines were assigned to the *Z* isomer of the amide group, while the downfield lines of the imine proton were attributed to the *E* isomer of compounds **6–11**. Lastly, two sets as a result of *cis/trans* amide conformers of the N-CH₂ signal were monitored at about

4.84 ppm and about 4.65 ppm for compounds **6–11**. The ^{13}C -NMR spectrum of compounds showed *cis/trans* conformers with two carbon signals around 45.9–47.9 and 46.7–48.3 ppm corresponding to the CH₂ group, and 161.7–162.9 and 162.9–164.0 ppm corresponding to the C=O group. In addition, two sets of signals were observed around 145.3–146.9 and 146.1–147.6 ppm, corresponding to -N=CH carbons owing to *E* and *Z* geometrical isomers. The content percentages have been calculated by using ^1H -NMR and ^{13}C -NMR data in each one. *Cis/trans* conformer and *E/Z* geometrical isomer structures of compounds **6–11** are given in Scheme 2. Furthermore, compounds **6–11** gave mass spectra and elemental analysis data compatible with certain structures.

It must be noted that the synthesis and glutathione reductase inhibitory properties of compounds **6** and **7** were previously published by our group.^[47] Different inhibitory effects for hCA I, hCA II, AChE, and BuChE due to different functional groups (-OH, -OCH₃, -NO₂, -CH₃, and -N(CH₃)₂) found in the structures of **6–11** Schiff base derivatives used in this study are shown. The values determined here indicate that there may be new classes of CAIs, in addition to sulfonamides, which are known to be potent inhibitors

of CA isoenzymes. These Schiff bases (6–11) obtained show that they are highly effective hCA I and hCA II inhibitors at low doses in these trials with the esterase method. The values determined in this study indicate the potential for compounds 6–11 to generate CAIs that may affect other untested CA isoenzymes. It has also been observed that these substances (6–11) are effective inhibitors of AChE and BuChE and may be candidates for use in the treatment of AD.

The biological activity data of 6–11 can be interpreted as follows; as they show effective inhibition of both CA isoenzymes and ChE enzymes, it may aid the development of new and more effective drug substances to reduce or improve the progression of AD. In addition to the comparison of these Schiff bases (6–11) synthesized in our study with reference molecules, we performed *in silico* studies to explore the interactions of compounds, specifically the ones with the best inhibition values with targets. These studies indicated that compounds could occupy the binding sites and form interactions with critical residues to inhibit the functions of targets. These results can be used to prepare more effective drug molecules for the treatment of diseases or to obtain drug precursors.

4 | EXPERIMENTAL

4.1 | Chemistry

4.1.1 | General information

General details of the synthesis of scaffolds of the compounds are detailed in our previous paper.^[25] Electric melting point apparatus Büchi was used to check and measure all melting points of the intermediate and final synthesized compounds. Characterization tests are conducted with different approaches. The ¹³C and ¹H NMR spectra were recorded at 100 and 400 MHz, respectively, using an Agilent Premium spectrometer in deuterated DMSO-*d*₆ with tetramethylsilane (TMS) as internal standard. The IR spectra were obtained on a Perkin Elmer Spectrum 100 FT-IR spectrometer. The elemental analyses were executed on a Carlo-Erba 1106 CHN analyzer. Heated electrospray ionization mass spectra were verified using a Thermo Scientific Quantum Access MAX Triple Stage Quadrupole mass spectrometer. Microwave-assisted reactions were carried out in a monomode CEM-Discover apparatus using 300 W maximum power.

The InChI codes of the investigated compounds, together with some biological activity data, are provided as Supporting Information.

4.1.2 | Synthesis of compound 4

Compound 3 (10 mmol, 2.47 g) and an equivalent amount of metallic sodium (10 mmol, 0.23 g) were mixed in 15 mL absolute ethanol. The reaction mixture was then irradiated with microwaves at 75°C for 3 min

in a 35 mL vial. After the acidic proton was released, (1.66 mL 15 mmol) ethyl bromoacetate was transferred to the reaction mixture and irradiated for another 3 min at 75°C. After the completion of the reaction (TLC, eluent AcOEt/hexane, 3:1), the solvent was evaporated under a vacuum. The solid product was recrystallized from water to obtain a pure structure. Yield 2.71 g (82%), mp 99–101°C (lit. 98–100).^[20]

4.1.3 | Synthesis of compound 5

In 35 mL microwave vial, compound 4 (1.66 g, 5 mmol) and (9.52 mL, 200 mmol) excess NH₂NH₂·H₂O (100% concentration) were dissolved in 10 mL absolute EtOH. The reaction solution was irradiated with microwaves at 60°C for 15 min. After the completion of the reaction (TLC, methanol) the reaction mixture was cooled to room temperature. The crude solid was filtered and recrystallized twice from ethanol. Yield (1.41 g, 93%), mp 216–218°C (lit. 215–217).^[20,48]

4.1.4 | General process for the preparation of Schiff base derivatives 6–11

Microwave Method: The solution of 1 mmol compound 5 and the corresponding 1 mmol aromatic aldehyde in 10 mL ethanol in the presence of a catalytic amount (2–3 drops) of glacial acetic acid (HOAc) was transferred in a 35 mL microwave vial. The reaction mixture was irradiated with microwave in the closed vials with pressure control at 120°C and 300 W for 5 min (hold time). After the completion of the reaction (by monitoring with TLC, Hexane: Ethylacetate, 1:3), the reaction mixture was cooled to room temperature until a crude solid appeared. The resulting solid was recrystallized two times from ethanol to obtain pure compounds 6–11. *Conventional Method:* The equivalent amount of compound 5 (1 mmol) and the corresponding aromatic aldehydes (1 mmol) were mixed in 30 mL ethanol in the presence of glacial acetic acid as a catalytic amount (two to three drops). The solution was stirred and refluxed overnight. The final procedures (work-up and purification) were carried on as described above.^[47,49] The spectroscopic and analytical data of compounds 6 and 7 can be found in Balaydin et al.^[47]

N'-(4-Hydroxy-2-methoxybenzylidene)-4-(1-[2-[2-(4-hydroxy-2-methoxybenzylidene)hydrazinyl]-2-oxoethyl]-3-methyl-5-oxo-1,5-dihydro-4H-1,2,4-triazol-4-yl)benzohydrazide (8): Yield: 0.45 g, (79%) (for conventional method), 0.48 g, (84%), (for microwave method), m.p. 235–237°C; Fourier-transform infrared (FTIR) spectroscopy (KBr): 3371 (OH), 3177 (NH), 3048 (Ar-CH), 2988 (Alip-CH), 1719 (C=O_{triazol}), 1681, 1670 (C=O_{hydrazide}), 1589 (C=N). ¹H NMR (400 MHz, DMSO-*d*₆) δ: 2.24 (s, 3H, CH₃), 3.52 (s, 6H, CH₃), 4.84 and 4.73 (s, 2H, CH₂, *cis* and *trans* conformers, *cis/trans* ratio 70/30), 6.97–7.73 (m, 10H, Ar-H), 7.92 (s, 1H, N=CH), 8.24 and 8.13 (s, 1H, N=CH, *E/Z* geometrical isomers, *E/Z* ratio 71/29), 9.61 (s, 2H, OH), 11.88, and 11.79 (s, 1H, NH, *cis* and *trans* conformers, *cis/trans* ratio 70/30), 12.03 (s, 1H, NH). ¹³C NMR (100 MHz, DMSO-*d*₆) δ: 12.7, 52.2 (CH₃), 47.1, and 47.6 (CH₂, *cis/trans*), 112.5, 113.2, 119.7,

121.0, 123.4, 124.9, 126.1, 127.0, 127.4, 129.1, 132.2, 133.7, 134.0, 134.9, 148.2, 152.4 (Ar.C), 144.2 (C=N), 145.0, 146.3, and 147.0 (N=CH, *E/Z*), 154.3, 162.6, and 164.0 (C=O, *cis/trans*), 166.7 (C=O). Calculated for C₂₈H₂₇N₇O₇: C 58.63, H 4.75, N 17.09; found %: C 58.59, H 4.76, N 17.11; Mass spectrum, *m/z* (*I*_{rel}, %): 574.3, [M+H]⁺ (100).

N'-[4-(Dimethylamino)benzylidene]-4-[1-(2-[4-(dimethylamino)benzylidene]hydrazineyl)-2-oxoethyl]-3-methyl-5-oxo-1,5-dihydro-4*H*-1,2,4-triazol-4-yl]benzohydrazide (**9**): Yield: 0.49 g, (86%) (for conventional method), 0.52 g, (91%), (for microwave method), m.p. 241–243°C; FTIR (KBr): 3208 (NH), 3047 (Ar-CH), 2979 (Alip-CH), 1721 (C=O_{triazol}), 1677, 1660 (C=O_{hydrazide}), 1587 (C=N). ¹H NMR (400 MHz, DMSO-*d*₆) δ: 2.17 (s, 3H, CH₃), 3.04 (s, 12H, N-CH₃), 4.91 and 4.69 (s, 2H, CH₂, *cis* and *trans* conformers, *cis/trans* ratio 71/29), 7.41–7.69 (m, 12H, Ar-H), 8.01 (s, 1H, NCH), 8.44 and 8.23 (s, 1H, N=CH, *E/Z* geometrical isomers, *E/Z* ratio 74/26), 11.68, and 11.74 (s, 1H, NH, *cis* and *trans* conformers, *cis/trans* ratio 73/27), 11.99 (s, 1H, NH). ¹³C NMR (100 MHz, DMSO-*d*₆) δ: 12.7 (CH₃), 41.6, 42.3 (CH₃), 46.3, and 47.2 (CH₂, *cis/trans*), 125.4, 126.1, 126.9, 127.9, 128.4, 129.4, 130.1, 132.0, 133.4, 134.6, 135.1, 149.4 (Ar.C), 143.4 (C=N), 145.4, 146.9, and 147.6 (N=CH, *E/Z*), 153.9, 162.9, and 163.2 (C=O, *cis/trans*), 166.5 (C=O). Calculated for C₃₀H₃₃N₉O₃: C 63.48, H 5.86, N 22.21; found %: C 63.51, H 5.84, N 22.19; Mass spectrum, *m/z* (*I*_{rel}, %): 568.4, [M+H]⁺ (100).

4-(3-Methyl-1-[2-[2-(4-methylbenzylidene)hydrazineyl]-2-oxoethyl]-5-oxo-1,5-dihydro-4*H*-1,2,4-triazol-4-yl)-*N'*-(4-methylbenzylidene)benzohydrazide (**10**): Yield: 0.40 g, (79%) (for conventional method), 0.43 g, (85%), (for microwave method), m.p. 250–252°C; FTIR (KBr): 3221 (NH), 3074 (Ar-CH), 2992 (Alip-CH), 1710 (C=O_{triazol}), 1677, 1660 (C=O_{hydrazide}), 1588 (C=N). ¹H NMR (400 MHz, DMSO-*d*₆) δ: 2.21 (s, 3H, CH₃), 2.38 (s, 3H, CH₃), 4.83 and 4.59 (s, 2H, CH₂, *cis* and *trans* conformers, *cis/trans* ratio 68/32), 7.59–7.71 (m, 10H, Ar-H), 7.95 (s, 1H, NCH), 7.99 (d, *J*=8.0 Hz, 2H, Ar-H), 8.40 and 8.20 (s, 1H, N=CH, *E/Z* geometrical isomers, *E/Z* ratio 71/29), 11.81, and 11.78 (s, 1H, NH, *cis* and *trans* conformers, *cis/trans* ratio 72/28), 12.00 (s, 1H, NH). ¹³C NMR (100 MHz, DMSO-*d*₆) δ: 13.5, 20.8 (CH₃), 45.9, and 46.7 (CH₂, *cis/trans*), 125.4, 126.0, 127.2, 127.9, 128.6, 129.4, 130.3, 132.5, 133.2, 133.9, 136.0, 137.1 (Ar.C), 141.4 (C=N), 143.1, 145.3, and 146.1 (N=CH, *E/Z*), 151.8, 162.6, and 162.9 (C=O, *cis/trans*), 166.5 (C=O). Calculated for C₂₈H₂₇N₇O₃: C 66.00, H 5.34, N 19.24; found %: C 65.96, H 5.33, N 19.25; Mass spectrum, *m/z* (*I*_{rel}, %): 510.14, [M+H]⁺ (100).

4-(3-Methyl-1-[2-[2-(3-methylbenzylidene)hydrazineyl]-2-oxoethyl]-5-oxo-1,5-dihydro-4*H*-1,2,4-triazol-4-yl)-*N'*-(3-methylbenzylidene)benzohydrazide (**11**): Yield: 0.41 g, (80%) (for conventional method), 0.47 g, (92%), (for microwave method), m.p. 245–247°C; FTIR (KBr): 3218 (NH), 3058 (Ar-CH), 2988 (Alip-CH), 1715 (C=O_{triazol}), 1680, 1671 (C=O_{hydrazide}), 1592 (C=N). ¹H NMR (400 MHz, DMSO-*d*₆) δ: 2.18 (s, 3H, CH₃), 2.41 (s, 3H, CH₃), 4.80 and 4.60 (s, 2H, CH₂, *cis* and *trans* conformers, *cis/trans* ratio 69/31), 7.48–7.79 (m, 12H, Ar-H), 7.94 (s, 1H, NCH), 8.27 and 8.12 (s, 1H, N=CH, *E/Z* geometrical isomers, *E/Z* ratio 69/31), 11.81, and 11.69 (s, 1H, NH, *cis* and *trans* conformers, *cis/trans* ratio 72/28), 12.01 (s, 1H, NH). ¹³C NMR (100 MHz, DMSO-*d*₆) δ: 12.9 (CH₃), 21.3 (CH₃), 47.9, and 48.3 (CH₂, *cis/trans*), 125.0, 126.4, 127.0,

128.2, 128.9, 129.7, 130.4, 131.0, 131.8, 132.6, 133.1, 133.9, 134.6, 135.6, 137.0, 138.2 (Ar.C), 144.0 (C=N), 145.0, 145.8, and 146.7 (N=CH, *E/Z*), 155.3, 161.7, and 162.9 (C=O, *cis/trans*), 166.8 (C=O). Calculated for C₂₈H₂₇N₇O₃: C 66.00, H 5.34, N 19.24; found %: C 66.02, H 5.34, N 19.20; Mass spectrum, *m/z* (*I*_{rel}, %): 510.27, [M+H]⁺ (100).

4.2 | Biological assays

4.2.1 | Purification of hCA I and II

hCA I and hCA II enzymes were obtained from fresh human erythrocytes using the method in our previous studies.^[7,8,50]

4.2.2 | Biological activities for hCA I and II

Biological activity analyses for human CA I and II isoenzymes were performed according to the protocol specified by Verpoorte et al.^[51] Inhibitory effects for compounds **6–11** were performed according to this method. The substances used in this study were tested in at least three replicates at each concentration. At least five different concentrations were used for each inhibitor. The activity was accepted as 100% in the measurement without inhibitor. Activity (%)-[Inhibitor] plots are plotted for each inhibitor. AZA was used as the reference inhibitor for both isoenzymes. The IC₅₀ values obtained for compounds **6–11** are summarized in Table 1.

4.2.3 | Biological activity measurement for ChEs

The inhibitory activities of AChE and BuChE enzymes for the tested compounds **6–11** were determined using the Ellman method.^[50] In our study, neostigmine was used as a reference inhibitor. The IC₅₀ values determined for compounds **6–11** are shown in Table 1.

4.3 | Molecular modeling studies

The studied compounds were sketched manually using the Maestro modeling program.^[52] All compounds were considered in four possible geometrical isomers as *E,E*, *E,Z*, *Z,E*, and *Z,Z* isomers depending on the relative positions of chemical groups attached to double bonds. The geometry optimizations of chosen hit molecules were carried out using the LigPrep module^[53] of Maestro with OPLS3e^[54] forcefield. The ionization state of the compounds was assigned to the physiological state (pH 7.4) using the Epik module^[55] of the Maestro molecular modeling package. Crystal structures of hCA I, hCA II, AChE, and BuChE were all retrieved from Protein Data Bank (PDB) with codes of 2FW4,^[56] 7BI5,^[57] 4EY5,^[58] and 4TPK,^[59] respectively. Using Protein Preparation Wizard^[60] of the Maestro program, all structures missing and/or mutated amino acids (if there were any) were corrected and bond orders of all atoms were

assigned. Small molecules and ions as well as water molecules that were not in the vicinity ($> 5 \text{ \AA}$) of the co-crystallized ligand were removed. Protonation states of amino acid residues were adjusted using PROPKA^[61] at physiological pH of 7.4.

GOLD docking program^[62,63] was used for initial pose prediction with the CHEMPLP scoring function. Binding sites were shaped by the residues within 10.0 \AA of the co-crystallized ligands. All water molecules were allowed to switch on and off (i.e., bound or displaced) as well as spin around the principal axis and translate up to 2.0 \AA . For each ligand/isomer, 100 poses were requested, and diverse solutions were generated with a cluster size of 10 and root mean square deviations (RMSD) up to 3.0 \AA . The ligand flexibility was achieved as in our previous study^[64] by flipping amide bonds (which allows *cis/trans* conformer switch, as shown in Scheme 2), flipping pyramidal and planar nitrogen atoms, and rotating protonated carboxylic acid groups as well as ring amine groups. Other settings were set as default.

After initial binding poses were generated for each ligand and isomers, the top docking poses for all studied ligands in complexes with target proteins were subjected to MD simulations with relaxation protocol applied so that clashes observed in the docking pose could be adjusted for 100 ns MD simulations. Desmond^[65] program was utilized for the MD simulations with the exact preparation steps and protocols followed as in our previous papers.^[64,66,67] MM/GBSA was used to calculate the FE of binding of each pose obtained by different docking fitness functions for each compound. The ranking of compounds relative to each other as well as between isomers of each ligand was performed based on the binding FE. Neostigmine for AChE and BuChE and AZA for hCA I and hCA II were considered as reference molecules in vitro tests and hence these molecules were also considered for molecular docking and MM/GBSA calculations. The reference compounds were also docked into the corresponding binding sites of target proteins after the compounds were prepared by LigPrep (i.e., same procedure as the preparation of studied molecules was applied). The docking poses of AZA at hCA I and hCA II binding sites were compared with known co-crystal structures as binding modes were well known (PDB codes 1AZM^[68] for hCA I and 3HS4^[69] for hCA II). The docked poses were well aligned to co-crystallized ones with RMSD values less than 2.0 \AA . MM/GBSA calculations were again performed for complexes of reference molecules with their respective target proteins after MD simulations.

ACKNOWLEDGMENTS

This study was supported by TÜBİTAK "The Scientific and Technical Research Council of Türkiye" for financial support through project number: 112T640. This study was also supported by the Scientific Research Project Unit of Istanbul Technical University Grant Number: 44790 and the Scientific Research Projects Commission of Bahçeşehir University, project numbers: BAP.2022-02.59 and BAP.2022-01.22.

CONFLICTS OF INTEREST STATEMENT

The authors declare no conflicts of interest.

DATA AVAILABILITY STATEMENT

The data that support the findings of this study are available from the corresponding author upon reasonable request.

ORCID

Musa Özil  <http://orcid.org/0000-0002-1980-1364>

Halis T. Balaydin  <http://orcid.org/0000-0003-2823-4004>

Berna Doğan  <http://orcid.org/0000-0002-9638-2896>

Murat Şentürk  <http://orcid.org/0000-0002-5650-5177>

Serdar Durdagi  <http://orcid.org/0000-0002-0426-0905>

REFERENCES

- [1] C. T. Supuran, *Nat. Rev. Drug Discov.* **2008**, *7*, 168.
- [2] M. F. Said, R. F. George, A. Petreni, C. T. Supuran, N. M. Mohamed, *J. Enzyme Inhib. Med. Chem.* **2022**, *37*(1), 701.
- [3] C. T. Supuran, A. Scozzafava, J. Conway, *Carbonic Anhydrase: Its Inhibitors And Activators*, 1, CRC Press, Boca Raton **2004**.
- [4] T. Arslan, Z. Biyiklioglu, M. Şentürk, *RSC Adv.* **2018**, *8*(19), 10172.
- [5] H. T. Balaydin, S. Durdagi, D. Ekinci, M. Şentürk, S. Göksu, A. Menzek, *J. Enzyme Inhib. Med. Chem.* **2012**, *27*(4), 467.
- [6] H. T. Balaydin, M. Şentürk, A. Menzek, *Bioorg. Med. Chem. Lett.* **2012**, *22*(3), 1352.
- [7] A. Innocenti, D. Vullo, A. Scozzafava, C. T. Supuran, *Bioorg. Med. Chem. Lett.* **2008**, *18*(5), 1583.
- [8] S. Işık, D. Vullo, S. Durdagi, D. Ekinci, M. Şentürk, A. Çetin, E. Şentürk, C. T. Supuran, *Bioorg. Med. Chem. Lett.* **2015**, *25*(23), 5636.
- [9] H. Ahmad, S. Ahmad, M. Ali, A. Latif, S. A. A. Shah, H. Naz, N. ur Rahman, F. Shaheen, A. Wadood, H. U. Khan, M. Ahmad, *Bioorg. Chem.* **2018**, *78*, 427.
- [10] R. Çakmak, E. Başaran, M. Şentürk, *Arch. Pharm.* **2022**, *355*(4), 2100430.
- [11] J. D. Ulrich, D. M. Holtzman, *ACS Chem. Neurosci.* **2016**, *7*(4), 420.
- [12] M. A. Telpoukhovskaia, B. O. Patrick, C. Rodríguez-Rodríguez, C. Orvig, *Bioorg. Med. Chem. Lett.* **2016**, *26*(6), 1624.
- [13] Y. Ünver, K. Sancak, F. Çelik, E. Birinci, M. Küçük, S. Soylu, N. A. Burnaz, *Eur. J. Med. Chem.* **2014**, *84*, 639.
- [14] A. Almasirad, S. A. Tabatabai, M. Faizi, A. Kebriaeezadeh, N. Mehrabi, A. Dalvandi, A. Shafiee, *Bioorg. Med. Chem. Lett.* **2004**, *14*(24), 6057.
- [15] R. Paprocka, M. Wiese, A. Eljaszewicz, A. Helmin-Basa, A. Gzella, B. Modzelewska-Banachiewicz, J. Michalkiewicz, *Bioorg. Med. Chem. Lett.* **2015**, *25*(13), 2664.
- [16] R. S. Upadhayaya, N. Sinha, S. Jain, N. Kishore, R. Chandra, S. K. Arora, *Bioorg. Med. Chem.* **2004**, *12*(9), 2225.
- [17] N. Kulabaş, E. Tatar, Ö. Bingöl Özakpınar, D. Özavcı, C. Pannecouque, E. De Clercq, İ. Küçükgüzel, *Eur. J. Med. Chem.* **2016**, *121*, 58.
- [18] B. Kahveci, M. Özil, M. Serdar, *Heteroat. Chem.* **2008**, *19*(1), 38.
- [19] A. Pinner, *Die imidoether und ihre Derivative*, 1. Auflage, *Oppenheim*, Berlin **1982**.
- [20] M. Özil, O. Bodur, S. Ülker, B. Kahveci, *Chem. Heterocycl. Compds.* **2015**, *51*(1), 88.
- [21] M. Özil, M. Canpolat, *Polyhedron* **2013**, *51*, 82.
- [22] R. M. Dawson, *Neurosci. Lett.* **1990**, *118*(1), 85.
- [23] X. Gao, C. Zhou, H. Liu, L. Liu, J. Tang, X. Xia, *J. Enzyme Inhib. Med. Chem.* **2017**, *32*(1), 146.
- [24] E. Akin Kazancioglu, M. Senturk, *Bioorg. Chem.* **2020**, *104*, 104279.
- [25] M. Özil, H. T. Balaydin, M. Şentürk, *Bioorg. Chem.* **2019**, *86*, 705.
- [26] G. Provensi, F. Carta, A. Nocentini, C. T. Supuran, F. Casamenti, M. B. Passani, S. Fossati, *Int. J. Mol. Sci.* **2019**, *20*(19), 4724.
- [27] A. Ozdemir, G. Turan-Zitouni, Z. A. Kaplancikli, Y. Tunali, *J. Enzyme Inhib. Med. Chem.* **2009**, *24*(3), 825.

- [28] E. Mete, B. Comez, H. Inci Gul, I. Gulcin, C. T. Supuran, *J. Enzyme Inhib. Med. Chem.* **2016**, 31(sup2), 1.
- [29] T. Arslan, G. Çelik, H. Çelik, M. Şentürk, N. Yaylı, D. Ekinci, *Arch. Pharm. (Weinheim)* **2016**, 349(9), 741.
- [30] T. Arslan, M. Buğrahan Ceylan, H. Baş, Z. Biyiklioglu, M. Senturk, *Dalton Trans.* **2020**, 49(1), 203.
- [31] R. Demirdağ, V. Çomaklı, M. Şentürk, D. Ekinci, Ö. İrfan Küfrevioğlu, C. T. Supuran, *Bioorg. Med. Chem.* **2013**, 21(6), 1522.
- [32] D. Ekinci, M. Al-Rashida, G. Abbas, M. Şentürk, C. T. Supuran, *J. Enzyme Inhib. Med. Chem.* **2012**, 27(5), 744.
- [33] M. Güney, H. Çavdar, M. Şentürk, D. Ekinci, *Bioorg. Med. Chem. Lett.* **2015**, 25(16), 3261.
- [34] S. Durdagi, N. Korkmaz, S. Isik, D. Vullo, D. Astley, D. Ekinci, R. E. Salmas, M. Senturk, C. Supuran, *J. Enzyme Inhib. Med. Chem.* **2016**, 31(6), 1214.
- [35] S. Durdagi, M. Şentürk, D. Ekinci, H. T. Balaydin, S. Göksu, Ö. İ. Küfrevioğlu, A. Innocenti, A. Scozzafava, C. T. Supuran, *Bioorg. Med. Chem.* **2011**, 19(4), 1381.
- [36] I. Fidan, R. E. Salmas, M. Arslan, M. Şentürk, S. Durdagi, D. Ekinci, E. Şentürk, S. Coşgun, C. T. Supuran, *Bioorg. Med. Chem.* **2015**, 23(23), 7353.
- [37] Z. Ö. Özdemir, M. Şentürk, D. Ekinci, *J. Enzyme Inhib. Med. Chem.* **2013**, 28(2), 316.
- [38] T. Arslan, N. Çakır, T. Keleş, Z. Biyiklioglu, M. Senturk, *Bioorg. Chem.* **2019**, 90, 103100.
- [39] N. Lemon, E. Canepa, M. A. Ilies, S. Fossati, *Front. Aging Neurosci.* **2021**, 13, 785.
- [40] N. Chiaramonte, M. Romanelli, E. Teodori, C. Supuran, *Metabolites* **2018**, 8(2), 36.
- [41] A. Maresca, C. Temperini, L. Pochet, B. Masereel, A. Scozzafava, C. T. Supuran, *J. Med. Chem.* **2010**, 53(1), 335.
- [42] A. Maresca, C. Temperini, H. Vu, N. B. Pham, S.-A. Poulsen, A. Scozzafava, R. J. Quinn, C. T. Supuran, *J. Am. Chem. Soc.* **2009**, 131(8), 3057.
- [43] C. Temperini, A. Innocenti, A. Scozzafava, S. Parkkila, C. T. Supuran, *J. Med. Chem.* **2010**, 53(2), 850.
- [44] J. Cheung, E. N. Gary, K. Shiomi, T. L. Rosenberry, *ACS Med. Chem. Lett.* **2013**, 4(11), 1091.
- [45] H. Bektas, A. Demirbas, N. Demirbas, S. A. Karaoglu, *Turk. J. Biol.* **2010**, 34(2), 165.
- [46] B. Kahveci, E. Menteşe, M. Özil, F. Yılmaz, M. Serdar, *J. Heterocycl. Chem.* **2016**, 53(3), 975.
- [47] H. T. Balaydin, M. Özil, M. Şentürk, *Arch. Pharm.* **2018**, 351(8), 1800086.
- [48] M. Özil, G. Tacal, N. Baltas, M. Emirik, *Lett. Org. Chem.* **2020**, 17(4), 309.
- [49] B. Kahveci, E. Menteşe, M. Özil, S. Ülker, M. Ertürk, *Monatsh. Chem. Chem. Month.* **2013**, 144(7), 993.
- [50] G. L. Ellman, K. D. Courtney, Andres Jr., V., R. M. Featherstone, *Biochem. Pharmacol.* **1961**, 7(2), 88.
- [51] J. A. Verpoorte, S. Mehta, J. T. Edsall, *J. Biol. Chem.* **1967**, 242(18), 4221.
- [52] Schrödinger Release 2018-1: Maestro, Schrödinger, LLC, New York, NY, **2018**.
- [53] Schrödinger Release 2018-1: LigPrep, Schrödinger, LLC, New York, NY, **2018**.
- [54] K. Roos, C. Wu, W. Damm, M. Reboul, J. M. Stevenson, C. Lu, M. K. Dahlgren, S. Mondal, W. Chen, L. Wang, R. Abel, R. A. Friesner, E. D. Harder, *J. Chem. Theory Comput.* **2019**, 15(3), 1863.
- [55] J. C. Shelley, A. Cholleti, L. L. Frye, J. R. Greenwood, M. R. Timlin, M. Uchimaya, *J. Comput.-Aided Mol. Des.* **2007**, 21(12), 681.
- [56] C. Temperini, A. Scozzafava, C. T. Supuran, *Bioorg. Med. Chem. Lett.* **2006**, 16(19), 5152.
- [57] G. De Simone, S. Bua, C. T. Supuran, V. Alterio, *Biochem. Biophys. Res. Commun.* **2021**, 548, 217.
- [58] J. Cheung, M. J. Rudolph, F. Burshteyn, M. S. Cassidy, E. N. Gary, J. Love, M. C. Franklin, J. J. Height, *J. Med. Chem.* **2012**, 55(22), 10282.
- [59] B. Brus, U. Košak, S. Turk, A. Pišlar, N. Coquelle, J. Kos, J. Stojan, J.-P. Colletier, S. Gobec, *J. Med. Chem.* **2014**, 57(19), 8167.
- [60] G. Madhavi Sastry, M. Adzhigirey, T. Day, R. Annabhimoju, W. Sherman, *J. Comput.-Aided Mol. Des.* **2013**, 27(3), 221.
- [61] D. C. Bas, D. M. Rogers, J. H. Jensen, *Proteins: Struct., Funct., Bioinf.* **2008**, 73(3), 765.
- [62] G. Jones, P. Willett, R. C. Glen, A. R. Leach, R. Taylor, *J. Mol. Biol.*, 267(3) **1997**, pp. 727.
- [63] M. L. Verdonk, G. Chessari, J. C. Cole, M. J. Hartshorn, C. W. Murray, J. W. M. Nissink, R. D. Taylor, R. Taylor, *J. Med. Chem.* **2005**, 48(20), 6504.
- [64] B. Dogan, S. Durdagi, *Mol. Inf.* **2021**, 40(2), e2000012.
- [65] K. J. Bowers, D. E. Chow, H. Xu, R. O. Dror, M. P. Eastwood, B. A. Gregersen, J. L. Klepeis, I. Kolossvary, M. A. Moraes, F. D. Sacerdoti In *Scalable algorithms for molecular dynamics simulations on commodity clusters*, SC'06: Proceedings of the 2006 ACM/IEEE Conference on Supercomputing, IEEE: **2006**; 43.
- [66] G. Tutumlu, B. Dogan, T. Avsar, M. D. Orhan, S. Calis, S. Durdagi, *Front. Chem.* **2020**, 8, 167.
- [67] D. Kanan, T. Kanan, B. Dogan, M. D. Orhan, T. Avsar, S. Durdagi, *ChemMedChem* **2021**, 16(3), 555.
- [68] S. Chakravarty, K. K. Kannan, *J. Mol. Biol.* **1994**, 243(2), 298.
- [69] K. H. Sippel, A. H. Robbins, J. Domsic, C. Genis, M. Agbandje-McKenna, R. McKenna, *Acta Crystallogr. Sect. F. Struct. Biol. Cryst. Commun.* **2009**, 65, 992.

SUPPORTING INFORMATION

Additional supporting information can be found online in the Supporting Information section at the end of this article.

How to cite this article: M. Özil, H. T. Balaydin, B. Dogan, M. Şentürk, S. Durdagi, *Arch. Pharm.* **2024**, e2300266.
<https://doi.org/10.1002/ardp.202300266>